

AC Susceptibility Measurements and Mechanical Performance of Bulk MgB₂

O. Ozturk · E. Asikuzun · S. Kaya · M. Erdem ·
S. Safran · A. Kilic · C. Terzioglu

Received: 26 December 2014 / Accepted: 23 January 2015 / Published online: 13 February 2015
© Springer Science+Business Media New York 2015

Abstract The effects of Ar ambient pressure (vacuum and 0, 10, and 20 B) and annealing times (0.5 and 1 h) on microstructural, superconducting, and mechanical properties of bulk superconducting MgB₂ are investigated. The samples are produced using the solid-state reaction method. X-ray diffraction (XRD) and scanning electron microscopy (SEM) measurements are performed for determination of the crystal structure and surface morphology of MgB₂ samples, respectively. The superconducting properties are studied by AC magnetic susceptibility measurements. Microhardness analyses are made using the Vickers microhardness test for determination of mechanical properties of all samples. Increasing the Ar pressure decreases the lattice

parameters and hence the average grain size. Increasing the annealing time results in larger lattice parameters and larger grain formation. The susceptibility measurements revealed a two-step transition which is reminiscent of granular superconductors. The intra-grain transition temperature is determined to be 38.4 K for all samples. The inter-grain transition temperature of 37.2 K is obtained for samples produced under Ar ambient pressure. The samples produced under Ar ambient pressure have better superconducting properties than the ones produced in vacuum. Increasing the annealing time under vacuum further decreases the superconducting properties probably due to Mg loss.

Keywords MgB₂ superconductors · XRD · SEM · Vickers microhardness · Susceptibility

O. Ozturk (✉) · E. Asikuzun · S. Kaya
Department of Physics, Arts and Science Faculty, Kastamonu
University, 37100 Kastamonu, Turkey
e-mail: oozturk@kastamonu.edu.tr

O. Ozturk · S. Kaya
Research and Application Center, Kastamonu University, 37100
Kastamonu, Turkey

M. Erdem · C. Terzioglu
Department of Physics, Arts and Science Faculty, Abant Izzet
Baysal University, 14280 Bolu, Turkey

S. Safran · A. Kilic
Department of Physics, Science Faculty, Ankara University, 06100
Ankara, Turkey

S. Safran · A. Kilic
Center of Excellence for Superconductivity Research, Ankara
University, Ankara, Turkey

1 Introduction

The attention of researchers has focused on MgB₂ after the discovery of superconductivity in this compound by Akimitsu in 2001 [1]. This compound is quite promising for large-scale practical applications due to its simple crystal structure, low electromagnetic anisotropy, long coherence length, high critical current value (J_c), and high upper critical field value (H_{c2}) [2–4]. Obtaining high-quality grain boundaries and high current density is important for applications such as magnet, cable, and energy technologies [5, 7]. Low-cost MgB₂ superconductors can be manufactured in different forms like bulk, powder, wire, tape, and thin film. The properties of produced material are closely related with preparative techniques and production conditions. In order to obtain MgB₂ superconductors with good

mechanical properties, many studies in literature focused on the optimization of the production conditions [8–14]. Ambient pressure plays an important role in the production of MgB_2 superconducting bulk samples [9]. AC magnetic susceptibility has become a popular technique over the recent years and its measurement allows determination of some useful superconducting properties of superconductors [15, 16]. Although there is a vast amount of work in the literature [17–20] on the magnetic response of high-temperature superconductors (HTSCs), the interpretation of AC susceptibility is model dependent and there are some controversial issues concerning the occurrence of the peak in the out-of-phase component of the susceptibility.

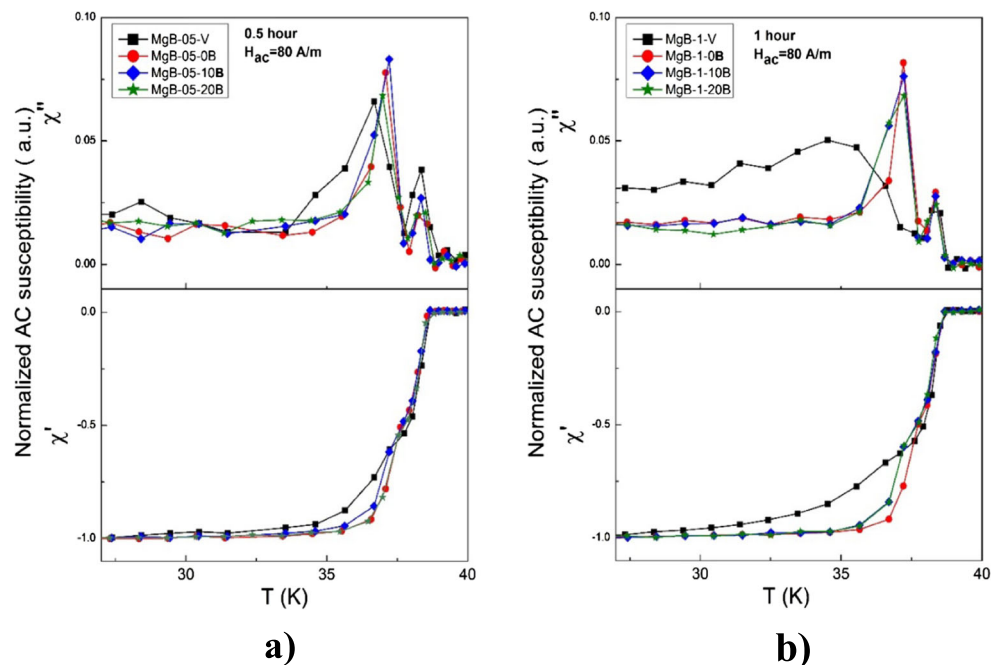
In the present study, the effects of argon pressure and annealing durations on the microstructural, superconducting, and mechanical properties of bulk MgB_2 samples are investigated. The ambient argon pressure is varied from vacuum to as high as 20 B. Annealing times of 0.5 and 1 h are used during the sample production. The microstructural, superconductivity, and mechanical properties of produced MgB_2 superconductors are determined with X-ray diffraction (XRD), scanning electron microscopy (SEM), susceptibility measurements, and Vickers microhardness tests, respectively. Other mechanical properties such as elastic modulus (E) and yield strength (Y) are also determined. Recently, when the all obtained results are analyzed, it is found that annealing time and applied pressure play an important role in the determination of the mechanical, superconducting, and microstructural properties of MgB_2 superconductor.

2 Experimental Techniques

In this study, MgB_2 powder (Alfa Aesar, -325 mesh, $<44 \mu\text{m}$) is used. Powder of 6 g is pressed into tablets with 13-mm diameter and 1.5-mm thickness, under the constant pressure of 7 tons. Bulk samples obtained by pressing are wrapped in the thallium (Ta) foil tightly to prevent oxidation and contamination during the heat treatment process. Material wrapped in Ta foil is placed directly into the steel tube. The air in steel pipe is evacuated using a vacuum apparatus, and the furnace is heated to 850°C from room temperature gradually with $5^\circ\text{C}/\text{min}$ heating and cooling rates. Samples are produced for 0.5 and 1 h of heat treatments. Similarly, 10 and 20 B Ar gas is introduced into the steel tube to produce samples under pressure. Hereafter, the produced samples will be denoted as MgB-05-V , MgB-05-0B , MgB-05-10B , MgB-05-20B , MgB-1-V , MgB-1-0B , MgB-1-10B , and MgB-1-20B .

The X-ray diffraction method is used to determine the crystal structure, the phases, and possible impurities. XRD measurements are performed using a Bruker D8 Advance model diffractometer with $\text{CuK}\alpha$ ($\lambda = 1.5405 \text{ \AA}$) radiation in the range $2\theta = 3^\circ - 90^\circ$ at a scan speed of $0.6^\circ/\text{min}$ at room temperature. XRD evaluation program is used for the determination of structure parameters and indexing of the peaks from the resulting pattern. The grain size, grain connectivity, and surface morphology of the sample are identified using a scanning electron microscope (JEOL 6390-LV), operated at 20 kV.

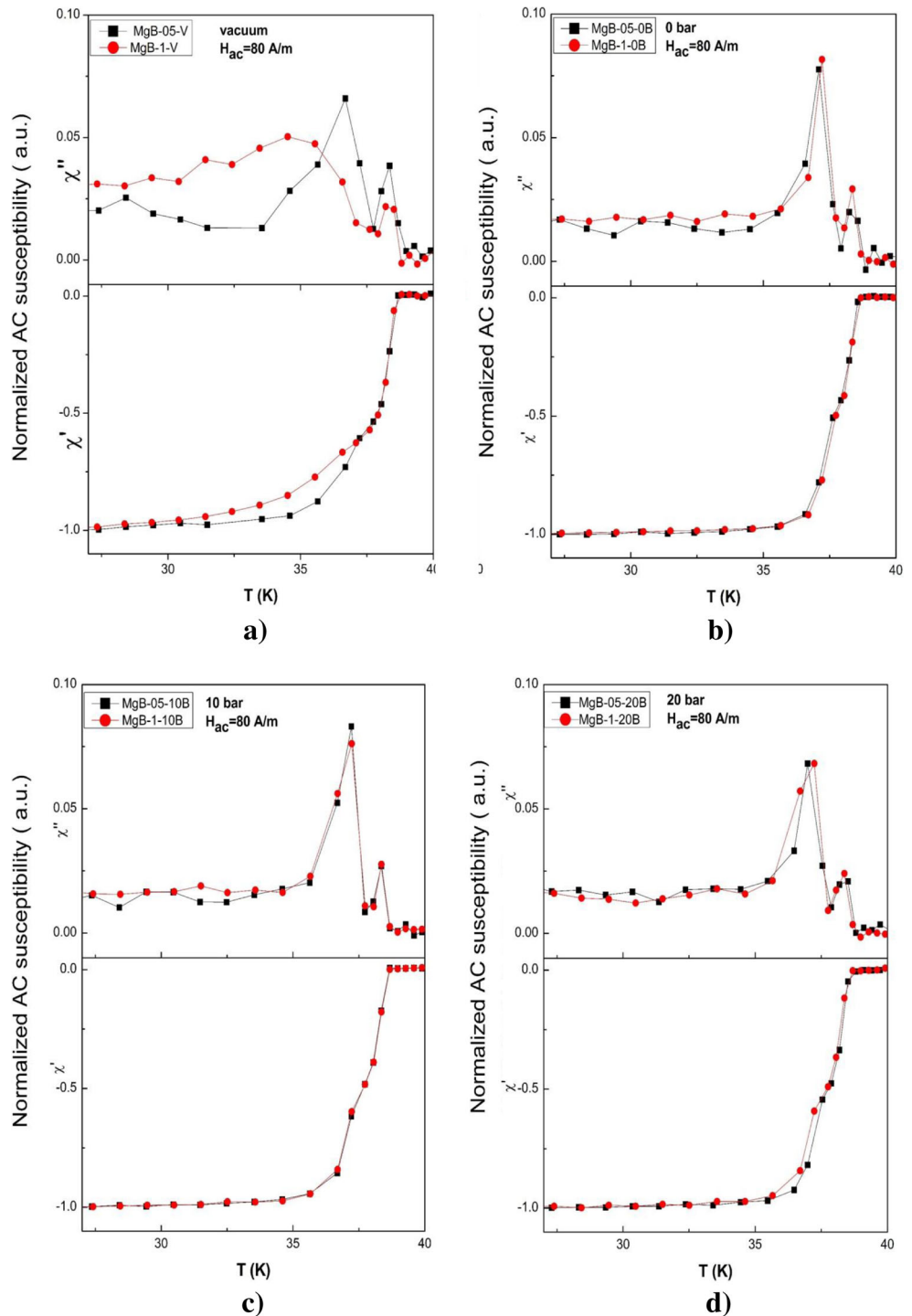
Fig. 1 Fundamental AC magnetic susceptibility as a function of temperature at $H_{\text{ac}} = 80 \text{ A/m}$ and frequency $f = 125 \text{ Hz}$. Duration of annealing is **a** 0.5 h and **b** 1 h in various pressure conditions



The susceptibility measurements are carried out by a commercial Lake Shore 7130-model AC susceptometer employing a mutual inductance coil system with a closed cycle refrigerator. The phase angle is adjusted in order to separate real and imaginary parts of the susceptibility. All the measurements reported in this paper are performed during warming, to make quantitative comparisons.

Vickers microhardness measurements of MgB₂ samples are performed by using digital microhardness tester (SHIMADZU HVM-2) at room temperature. Vickers diamond indenter is applied on the surface of the samples using various loads of 0.245, 0.490, 0.980, 1.960, and 2.940 N, and diagonal lengths of the traces formed on the surfaces of the samples are measured. Ten measurements are taken for each

Fig. 2 The normalized AC susceptibility curves of the samples with different annealing times as a function of temperature. The ambient is are **a** vacuum, **b** 0 B Ar, **c** 10 B Ar, and **d** 20 B Ar



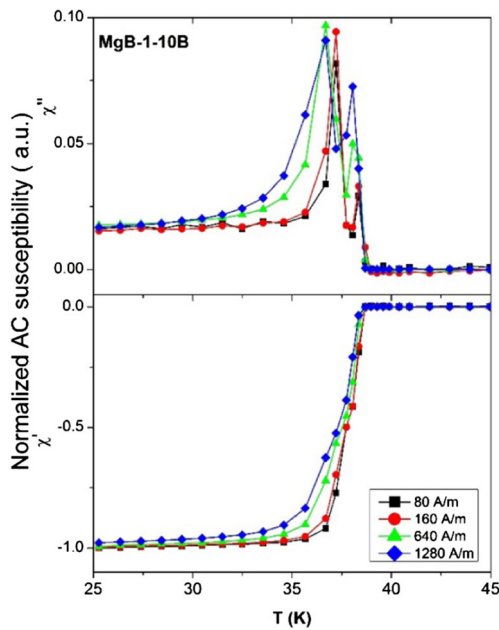


Fig. 3 AC susceptibility curves of MgB-1-10B sample as a function of temperature with varying AC fields

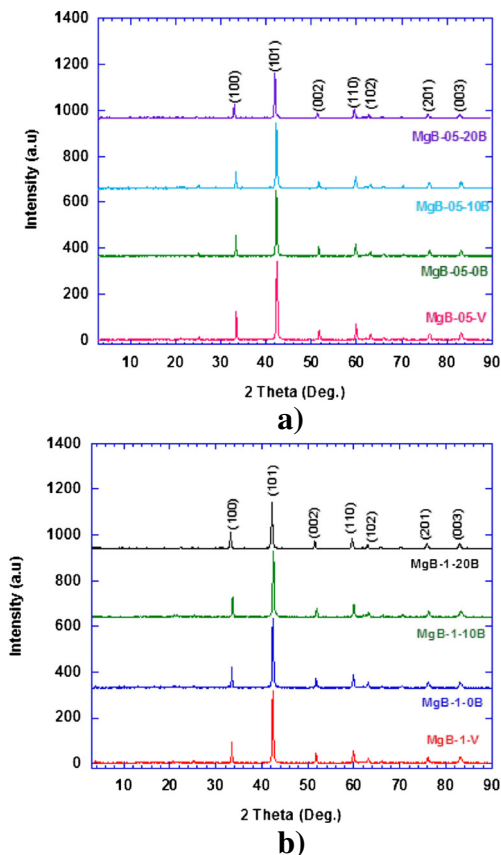


Fig. 4 XRD patterns of the samples **a** for 0.5-h annealing time and **b** for 1-h annealing time

load value and Vickers hardness values are calculated by taking their averages.

3 Results and Discussion

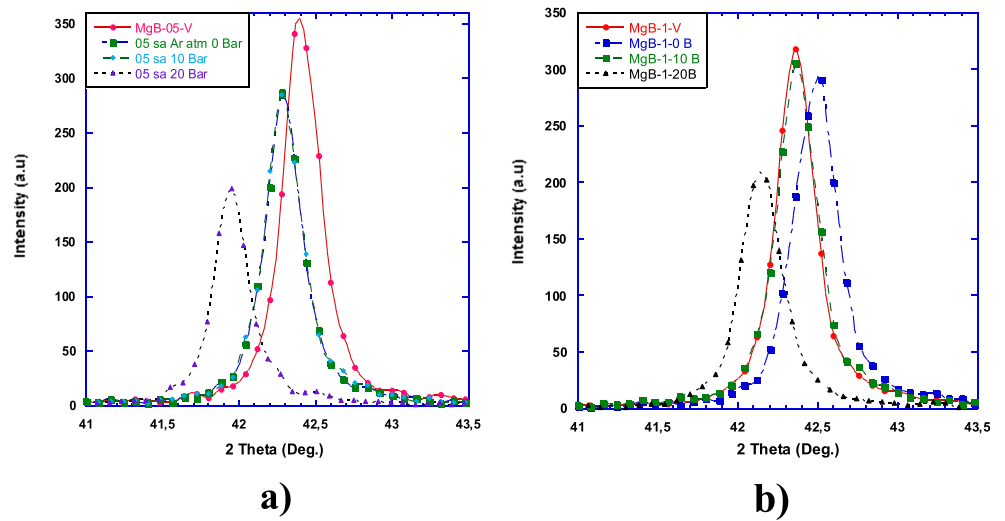
3.1 AC Susceptibility Measurements

AC susceptibility measurement is widely used as a non-destructive method for determination and characterization of the intra-grain and inter-grain features of the high-temperature superconductors [21–23]. The in-phase component of fundamental susceptibility, χ' , shows two significant drops as the temperature is decreased below T_c for granular superconductors. The first drop near T_c corresponds to intrinsic properties of grains. Another drop at lower temperatures indicates gradual changes associated with the occurrence of bulk superconductivity, where superconducting currents flow from grain to grain. The out-of-phase component, χ'' , generally exhibits a peak with decreasing temperature below T_c , which is attributed to the absorption of magnetic energy of the superconductor from the AC field. Therefore, χ' is proportional to the amount of flux penetration into the body of the superconductor, while χ'' is associated with AC losses in the mixed state of superconductor. In Fig. 1, the measurements of normalized AC susceptibility versus temperature for 0.5- and 1-h samples are plotted for AC fields of 80 A/m with $f = 125$ Hz. As expected for granular superconductors, for all samples, the transition takes place in two steps in χ' accompanied by two peaks in χ'' . When samples are cooled down under T_c , the grains become superconducting first, and shielding of the applied field is performed by intra-grain currents. On further lowering the temperature, the inter-grain current is developed. The intra-grain transition temperature is determined to be about 38.4 K for all samples. A similar behavior is observed for the inter-grain transition for all samples. The

Table 1 Calculated values of lattice parameters a and c and grain sizes of the samples

Samples	a (Å)	c (Å)	Grain size (nm)
MgB-05-V	3.098	3.52	36.86
MgB-05-0B	3.096	3.51	35.76
MgB-05-10B	3.096	3.50	34.27
MgB-05-20B	3.092	3.50	31.57
MgB-1-V	3.099	3.53	38.94
MgB-1-0B	3.098	3.53	36.05
MgB-1-10B	3.097	3.52	35.15
MgB-1-20B	3.093	3.50	32.14

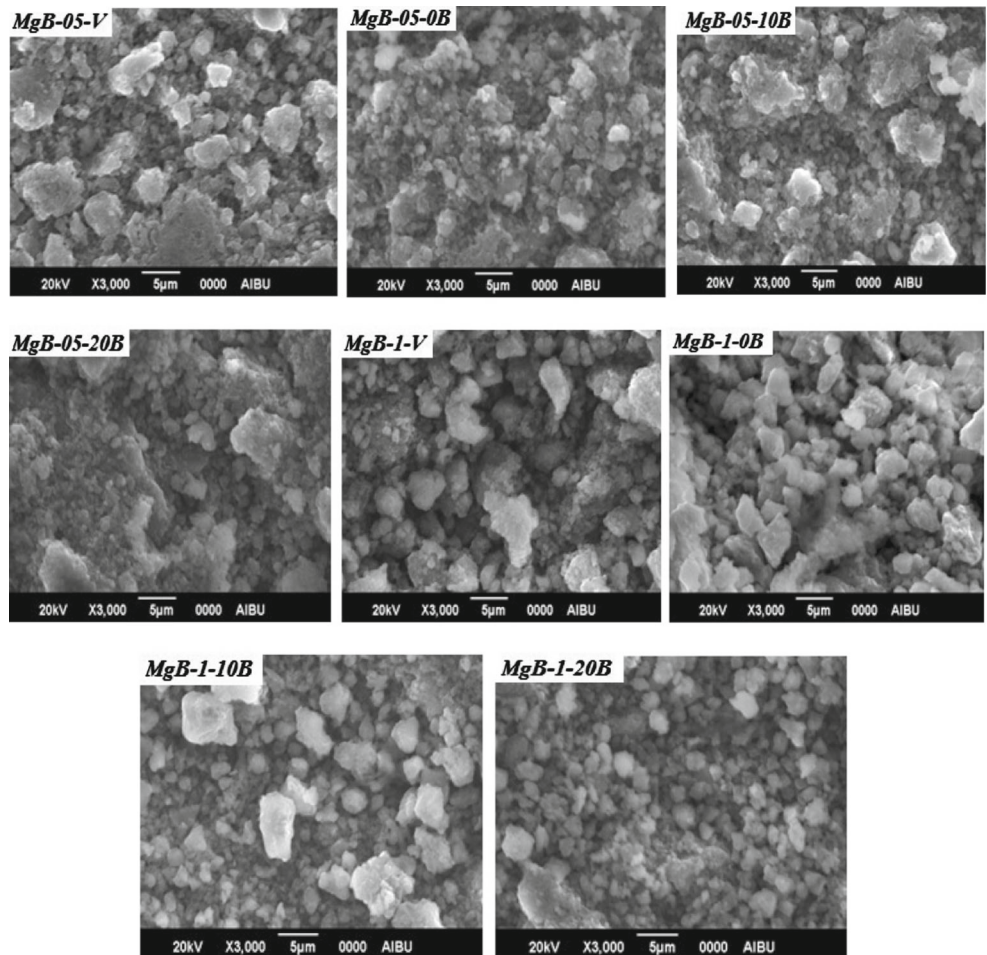
Fig. 5 Variation of (101) peaks with annealing ambient pressure **a** for 0.5-h annealing time and **b** for 1-h annealing time



inter-grain transition temperature is about 37.2 K for samples annealed in argon ambient pressure. The inter-grain transition temperature drops for vacuum annealed samples, namely, to 35.6 K for 0.5-h annealing and to 34.4 K for 1-h

annealing. During the annealing process at high temperature in vacuum environment, Mg can be lost due to the low boiling temperature of Mg. Therefore, the samples named MgB-05-V and MgB-1-V have broader magnetic transition

Fig. 6 SEM micrographs of the samples



when compared the other samples. The effect of the loss in Mg is more pronounced for MgB-1-V sample which is annealed for 1 h. Another possibility of the decrease in inter-grain temperature is due to the worsening of granular connectivity in the samples. Since the samples are produced under vacuum, the compactness and grain connectivity are not as high as for the samples produced under Ar ambient pressure. The pressure applied by Ar gas increases the compactness of the grains. The other three samples in each set have similar behavior in the AC susceptibility curves.

To clearly see the effects of annealing time and ambient pressure on the superconducting properties of the samples, the normalized AC susceptibility curves in Fig. 2 are plotted. The effect of annealing time is significant only in vacuum environment. The other samples do not show any significant changes. When annealing time increased from 0.5 to 1 h, the magnetic transition is broadened due to the reasons explained above.

Plot of real (χ') and imaginary (χ'') components of AC susceptibility as a function of temperature for MgB-1-10B sample at applied AC field amplitudes H_{ac} , ranging from 80 to 1280 A/m at a frequency $f = 125$ Hz are given in Fig. 3. When H_{ac} is increased from 80 to 1280 A/m, the peak height in χ'' increased and moved to lower temperatures slightly. This shows that AC losses increase with increasing field as expected. A similar behavior is also observed for other samples.

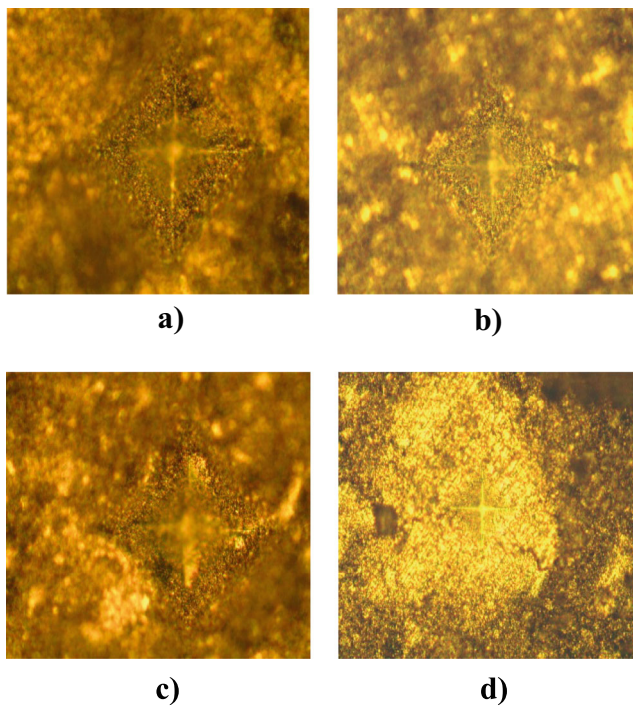


Fig. 7 The optical trace photos under 2.940 N load for the samples: **a** MgB-05-V, **b** MgB-05-0B, **c** MgB-05-10B, and **d** MgB-05-20B

3.2 XRD Analyses

X-ray diffraction patterns of the samples are given in Fig. 4. The XRD patterns of the samples belong to the MgB₂ main phase. There are no impurity phases in the samples. For both series, the peak intensities of samples produced in the vacuum ambient pressure are higher and peak widths are relatively narrower than others. The peak intensities decrease and the peak widths increase with the introduction and increasing the applied Ar pressure. The reason of this decrease in peak intensities may be a reduction of grain sizes with applied pressure. The lattice parameters a and c are calculated using XRD peaks and the results are shown in Table 1.

As seen from Table 1, the lattice parameters a and c decrease in transition from vacuum to Ar ambient pressure and by increasing Ar pressure. In literature, it is confirmed that the applied pressure decreases the values of a and c lattice parameters by shortening the length of MgB₂ bond [23–26].

The detailed XRD peak belonging to the (101) plane is shown in Fig. 5. The peaks shift to smaller angles with transition to Ar atmosphere from the vacuum environment and increasing the pressure in MgB-05 samples. This shift also confirms the decrease in c parameter [27]. Moreover, the change in the c lattice parameter is more than that of the a lattice parameter. This anisotropic behavior is due to the

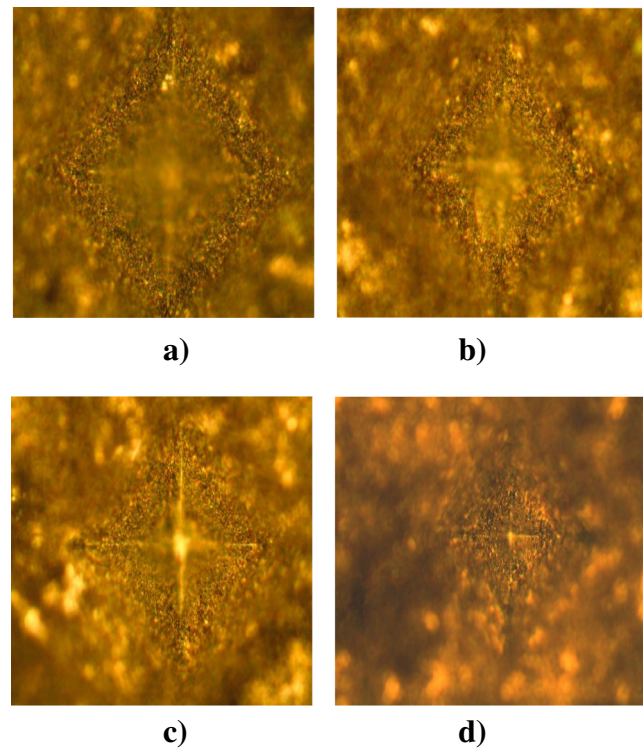


Fig. 8 The optical trace photos under 2.940 N load for the samples: **a** MgB-1-V, **b** MgB-1-0B, **c** MgB-1-10B, and **d** MgB-1-20B

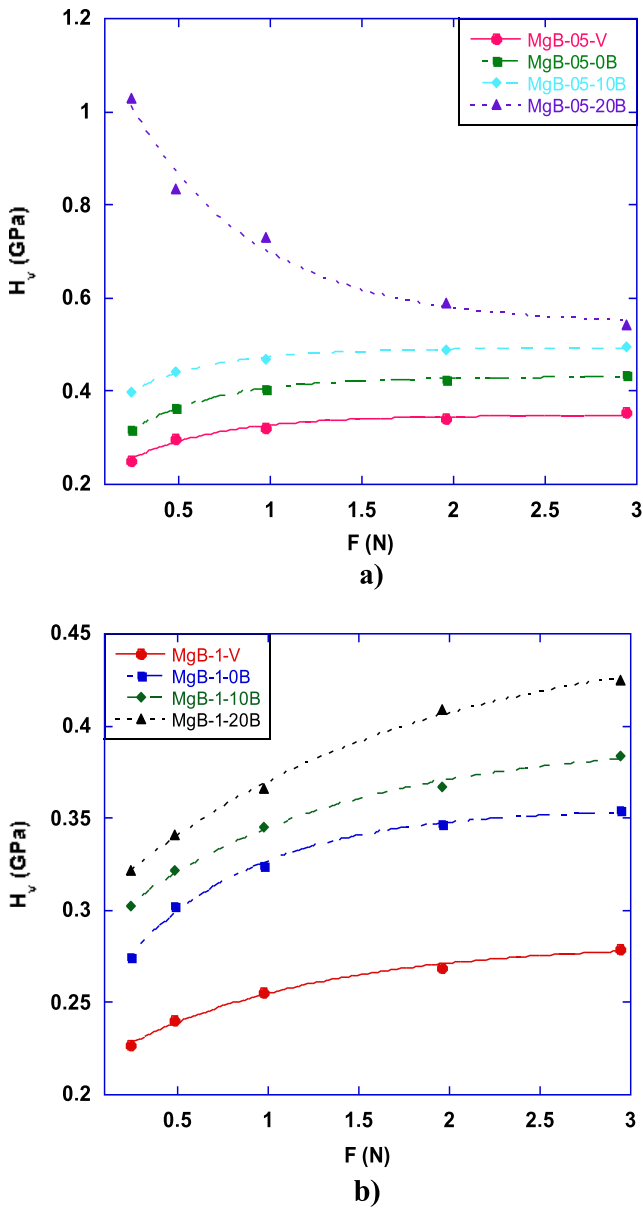


Fig. 9 The variations of microhardness with load for the samples **a** for 0.5-h annealing time and **b** for 1-h annealing time

difference in the bond strengths along *a* and *c* directions in MgB₂. The covalent *B – B* bonds along the *a* direction are stronger than the *Mg-B* ionic bonds along the *c* direction [28].

When the lattice parameters of the 0.5- and 1-h annealed samples are compared, it can be seen that the *a* and *c* lattice parameters of the samples exposed to heat treatment for 1 h are greater. This situation can be explained by increased thermal expansion occurring in samples with increasing heat treatment time. These results are confirmed by SEM images. The particle sizes of samples are calculated using the Warren-Scherer formula and are given in Table 1. As seen from the table, MgB-05-V and MgB-1-V

Table 2 Calculated values of *H_v*, *E*, and *Y* for the samples under varying applied loads

Samples	Load (N)	<i>H_v</i> (GPa)	<i>E</i> (GPa)	<i>Y</i> (GPa)
MgB-05-V	0.245	0.252	20.654	0.084
	0.490	0.279	22.867	0.093
	0.980	0.322	26.392	0.107
	1.960	0.341	27.949	0.113
	2.940	0.353	28.933	0.117
MgB-05-0B	0.245	0.316	25.900	0.105
	0.490	0.366	29.998	0.122
	0.980	0.404	33.113	0.134
	1.960	0.425	34.834	0.141
MgB-05-10B	0.245	0.398	32.621	0.132
	0.490	0.443	36.309	0.147
	0.980	0.469	38.440	0.156
	1.960	0.488	40.080	0.162
MgB-05-20B	0.245	0.499	40.890	0.166
	0.490	1.090	84.340	0.343
	0.980	0.833	68.275	0.277
	1.960	0.729	59.751	0.243
MgB-1-V	0.245	0.227	18.605	0.075
	0.490	0.240	19.671	0.080
	0.980	0.255	20.900	0.085
	1.960	0.269	22.048	0.089
MgB-1-0B	0.245	0.275	22.539	0.091
	0.490	0.302	24.752	0.100
	0.980	0.324	26.556	0.108
	1.960	0.347	28.441	0.115
MgB-1-10B	0.245	0.354	29.015	0.118
	0.490	0.322	26.392	0.107
	0.980	0.345	28.277	0.115
	1.960	0.367	30.080	0.122
MgB-1-20B	0.245	0.384	31.473	0.128
	0.490	0.322	26.392	0.107
	0.980	0.341	27.949	0.113
	1.960	0.366	29.998	0.122
MgB-1-20B	0.245	0.409	33.523	0.136
	0.490	0.425	34.834	0.141
	0.980	0.409	33.523	0.136
	1.960	0.425	34.834	0.141

samples have the greatest particle sizes of 36.86 and 38.94 nm, respectively. The particle sizes decrease with increasing the applied pressure. When the Ar pressure reaches to 20 B, the particle sizes of MgB-05-20B and MgB-1-20B samples decrease to 31.57 and 32.14 nm, respectively. In addition, we can say from the Table 1 that, the particle size of MgB-1 series is greater than the particle size of MgB-05 series.

As a result, particle sizes of the samples exposed to more heat treatment are greater. This condition is consistent with previous studies [29].

3.3 SEM Analysis

The SEM images of MgB₂ samples at 3000 magnification are shown in Fig. 6. Based on SEM photographs, it is determined that the samples exhibit a granular structure that is characteristic morphology of MgB₂ samples. In this granular structure, the grain sizes are different from each other, and partly, lumps are observed. Moreover, there is no specific orientation of particles. We see that the grain sizes of samples produced at 1 h are greater prominently. As is known, the particle size of material increases with increasing the heat treatment time and heat treatment temperature [27]. Besides, particle size decreases with increasing the pressure applied for each series. It can be said that voids between particles decrease with decreasing the particle size (especially for MgB-05-20B and MgB-1-20B) and so a stronger particle connection is obtained. The reduction of

particle size directly affects the mechanical properties of samples due to the decrease of porosity.

3.4 Vickers Microhardness Measurements

The Vickers microhardness test is used for determination of hardness values of MgB₂ samples produced in this study. Vickers hardness test is developed to measure the hardness of materials as an alternative to the Brinell method by Robert L. Smith and George E. Sandland in 1921. The Vickers test is easier than the other tests because required calculations are independent of the size of indenter. The Vickers microhardness value can be calculated by the following formula [30]:

$$H_v = \frac{F}{A} \approx \frac{1854.4F}{d^2} \text{ (GPa)} \quad (1)$$

The optical trace photos of the indentations for each sample under 2940 N load are shown in Figs. 7 and Fig. 8.

Figure 9 shows changes of the microhardness values as a function of applied load. The hardness values calculated

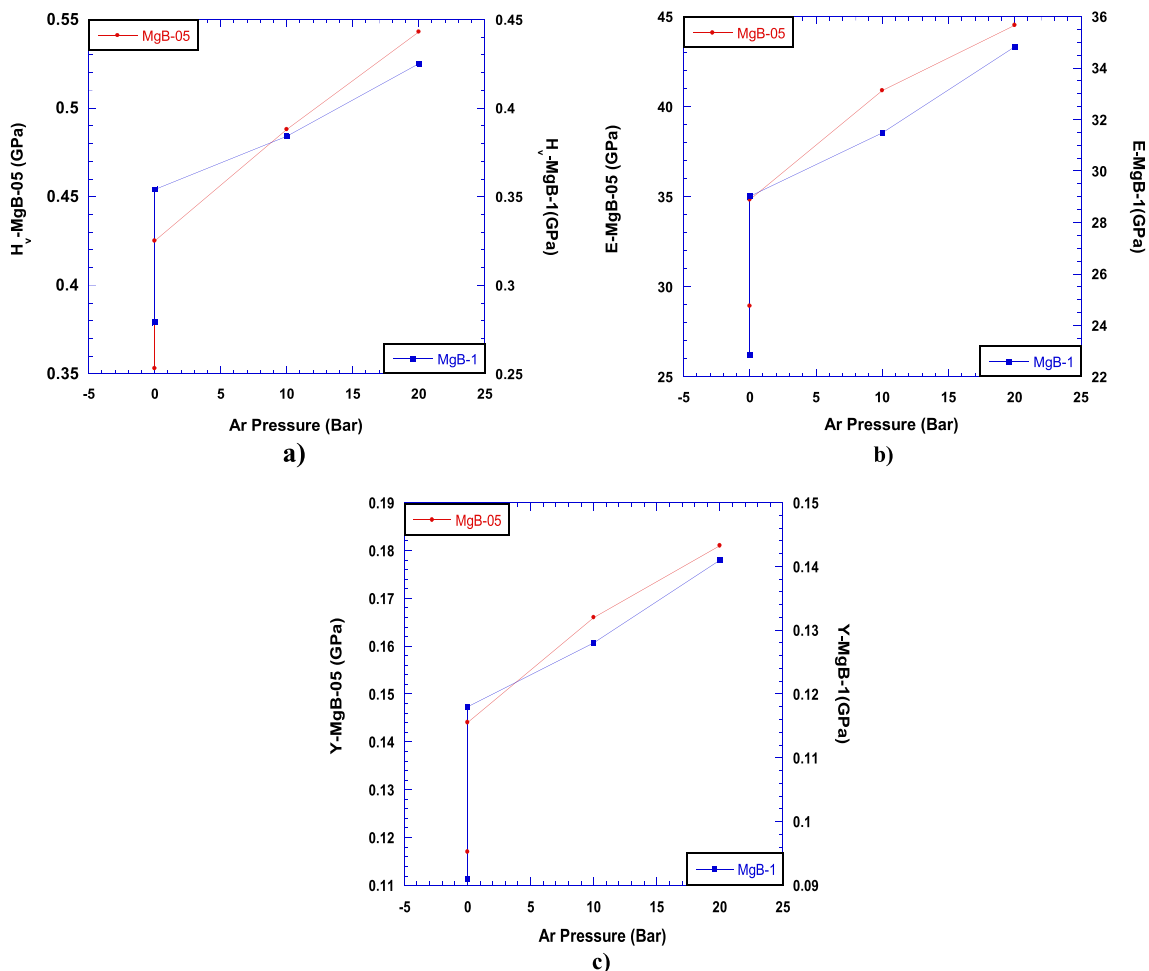


Fig. 10 The variations of **a** H_v , **b** E , and **c** Y with Ar pressure of the sample annealed for 0.5 h

using (1) are given in Table 2. We see that the microhardness values of the samples depend on the applied load. Microhardness values of all samples excluding the MgB-05-20B increase with applied load and they saturate to a plateau of constant hardness. At this plateau, the load-independent hardness values are reached. This behavior is called reverse indentation size effect (RISE) behavior in the literature. The microhardness of MgB-05-20B sample decreases with increasing the applied load. This sample exhibits the indentation size effect (ISE) behavior. From the table, it can be seen that the samples produced in 0.5 h have higher hardness values than the samples produced in 1 h. Moreover, the hardness values of the samples increase with ambient Ar pressure. Higher Ar pressure causes densification of the grains and reduction of the voids in the samples. The decrease of porosity and grain sizes together with higher densification results in harder samples.

Parameters such as modulus of elasticity (E) and yield strength (Y) that are as important as hardness to mechanical characterizations of materials [31–34] are also calculated, and values of these parameters are given in Table 2.

As can be seen from the table, elastic modulus (E) and yield stress (Y) values of the materials produced in Ar atmosphere are higher than the materials produced in vacuum ambient pressure in 0.5 h. The increase of hardness H_v , elastic modulus E , and yield stress Y values with the onset and increase of Ar pressure is plotted in Fig. 10. Moreover, E and Y values in MgB-05-V, MgB-05-0B, and MgB-05-10B samples increased with increasing applied load. However, these values decreased with the increase of the applied load in the MgB-05-20B sample. This result is related to the ISE behavior.

One can see that E and Y values of the samples produced in 1 h are lower than those of materials produced in 0.5 h. Herein, E and Y values of the samples produced at vacuum ambient pressure are less than those of samples produced at Ar atmosphere without pressure. The E and Y values increase with the applied pressure reaching to 10 and 20 B.

4 Conclusion

In this study, the microstructural, superconducting, and mechanical properties of MgB₂ superconductors produced at four different ambient conditions (vacuum and 0, 10, and 20 B) and annealing times of 0.5 and 1 h are analyzed. The following results are obtained:

- The lattice parameters a and c decrease when ambient Ar pressure increases. Increasing the annealing duration increases the lattice parameters. This result is consistent with the results in the literature because it is known that pressure has a shortening effect on the distances between the bonds.
- Reduction in grain sizes is observed with increasing Ar pressure. The decrease of grain sizes correlates with the decrease in lattice parameters. When the 0.5- and 1-h annealed samples are compared, it is seen that longer annealing causes larger grain formation along with higher lattice parameters.
- The characteristic morphology of granular structure of MgB₂ is observed by SEM images. The above results are confirmed by SEM images.
- According to the AC susceptibility measurements, the intra-grain transition temperature is determined to be about 38.4 K for all samples. The inter-grain transition temperature of 37.2 K is obtained for samples annealed in Ar ambient pressure. The inter-grain transition temperature drops for vacuum annealed samples, namely to 35.6 K for 0.5-h annealing and to 34.4 K for 1-h annealing. During the annealing process at high temperature in vacuum environment, Mg can be lost due to the low boiling temperature of Mg. Therefore, the samples named MgB-05-V and MgB-1-V have broader magnetic transition when compared the other samples. The effect of the loss in Mg is more pronounced for MgB-1-V sample which is annealed for 1 h.
- In addition, when the annealing time is increased from 0.5 to 1 h, the magnetic transition is broadened. It is considered to be due to Mg lost because of longer annealing time.
- According to Vickers microhardness measurements, the hardness of the samples is all load dependent. Apart from MgB-05-20B sample, the hardness of all samples increased with increasing applied loads which is known as RISE. The hardness of the MgB-05-20B sample decreased with increasing load showing ISE. The hardness values of the samples increase with increasing Ar pressure. Higher pressure causes better connection and densification of the samples. The samples produced in 0.5 h are found to be harder than the samples produced in 1 h. This result may be related with increasing the voids in the samples due to increasing annealing time.

Acknowledgments This research has been supported by the Kastamonu University Scientific Research Projects Coordination Department under the Grant No. KUBAP-03/2012-03.

References

1. Akimitsu, J., et Al.: Nature **410**, 63 (2001)
2. Buzea, C., Yamashita, T.: Supercond. Sci. Technol. **14**, 11 (2001)
3. Angst, M., Puzniak, R.: Condensed matter arXiv:0305048v2 (2003)
4. Larbalestier, D.C., Rike, M.O.L., Cooley, L.D., Polyanskii, A.A., Jiang, Y.J., Patnaik, S., Cai, X.Y., Feldmann, D.M., Gurevich, A.,

- Squitieri, A.A., Naus, M.T., Eom, C.B., Hellstrom, E.E., Cava, R.J., Regan, K.A., Rogado, N., Hayward, M.A., He, T., Slusky, J.S., Khalifah, P., Inumaru, K., Haas, M.: *Nature* **410**, 186–189 (2001)
5. Aksan, M.A., Yakıncı, M.E.: Güldeste, A.: *J. Alloy. Comp.* **424**, 33–40 (2006)
 6. Eyidi, D., Eibl, O., Wenzel, T., Nickel, K.G., Giovannini, M., Saccone, A.: *Micron* **34**, 85–86 (2003)
 7. Schmidt, J., Schnelle, W., Grin Y., Kniep, R.: *Solid State Sci.* **5**, 535–539 (2003)
 8. Kölemen, U.: *J. Alloy. Comp.* **425**, 429–435 (2006)
 9. Prikhna, T., Gawalek, W., Savchuk, Y., Sergienko, N., Moshchil, V., Dub, S., Sverdun, V., Kovalev, L., Penkin, V., Zeisberger, M., Wendt, M., Fuchs, G., Habisreuther, T., Litzkendorf, D., Nagorny, P., Melnikov, V.: *Phys. C*, 460–462 (2007)
 10. Dancera, C.E.J., Mikheenkob, P., Bevanb, A., Abellb, J.S., Todda, R.I., Grovenor, C.R.M.: *J. Eur. Ceram. Soc.* **29**, 1817–1824 (2009)
 11. Gorur, O., Nursoy, M., Terzioglu, C., Varilci, A., Belenli, I.: *J. Phys: Conf. Ser.* **153**, 012012 (2009)
 12. Güçlü, N.: *Mater. Chem. Phys.* **101**, 470–474 (2007)
 13. Kitaguchi, H., Kumakura, H., Togano, K.: *Phys. C: Supercond.* **363**, 198–201 (2001)
 14. Goldacker, W., Schlachter, S.I., Reiner, J., Zimmer, S., Nyilas, A., Kiesel, H.: *Appl. Supercond.* **13**, 3261–3264 (2003)
 15. Ozturk, O.: PhD Thesis, The effect of Au diffusion-doped on structural, superconducting and mechanical properties of $\text{Bi}_{1.8}\text{Pb}_{0.35}\text{Sr}_{1.9}\text{Ca}_{2.1}\text{Cu}_3\text{O}_y$ (2007)
 16. Aksu, E., Gencer, A., Calınlı, N., Koralay, H., Çavdar, S.: *Phys. B: Condens. Matter* **363**, 158–165 (2005)
 17. Goldfarb, R.B., Lelental, M., Thompson, C.A., Hein, R.A., Francavilla, T.L., Liebenberg, D.H. Plenum, New York (1992)
 18. Supple, F., Campbell, A.M., Cooper, J.R.: *Phys. C* **242**, 233 (1995)
 19. Flippin, R.B., Askew, T.R., Fendrich, J.A., Vlcek, B.M.: *Phys. C* **228**, 85 (1994)
 20. Caplin, A.D., Cohen, L.F., Perkins, G.K., Zhukov, A.A.: *Supercond. Sci. Technol.* **7**, 412 (1994)
 21. Chen, D.-X., Mei, Y.u., Luo, H.L.: *Phys. C* **167**, 317–323 (1990)
 22. Celebi, S., Kolemen, U., Malik, A.I., Ozturk, A.: *Phys. Status. Solidi A* **194**, 260–270 (2002)
 23. Gencer, A., Mutlu, R.H., Belenli, I., Ozogul, O., Aydmuraz, A.: *Supercond. Sci. Tech.* **9**, 284 (1996)
 24. Jorgensen, J.D., Hinks, D.G., Short, S.: *Phys. Rev. B* **63**, 224522 (2001)
 25. Vogt, T., Schneider, G., Hriljac, J.A., Yang, G., Abell, J.S.: *Phys. Rev. B* **63**, 220505 (2001)
 26. Zhang, C., Zhang, X.: *Comput. Mater. Sci.* **50**, 1097–1101 (2011)
 27. Ozturk, O., Asikuzun, E., Erdem, M., Yildirim, G., Yildiz, O., Terzioglu, C.: *J. Mater. Sci. Mater Electron* **23**, 511–519 (2012)
 28. Schneider, T., Di Castro, D.: *Phys. Rev. B* **72**, 054501 (2005)
 29. Dogruer, M., Gorur, O., Zalaoglu, Y., Ozturk, O., Yildirim, G., Varilci, A., Terzioglu, C.: *J. Mater. Sci. Mater Electron* **24**, 352–361 (2013)
 30. Koralay, H., Hicyilmaz, O., Cavdar, S., Asikuzun, E., Tasci, A.T., Ozturk, O.: *J. Mater. Sci. Mater Electron* **25**, 3116–3126 (2014)
 31. Arda, L., Ozturk, O., Asikuzun, E., Ataoglu, S.: *Powder Technol.* **235**, 479–484 (2013)
 32. Tosun, M., Ataoglu, S., Arda, L., Ozturk, O., Asikuzun, E., Akcan, D., Cakiroglu, O.: *Mater. Sci. Eng. A* **590**, 416–422 (2014)
 33. Asikuzun, E., Ozturk, O., Cetinkara, H.A., Yildirim, G., Varilci, A., Yilmazlar, M., Terzioglu, C.: *J. Mater. Sci. Mater Electron* **23**, 1001–1010 (2012)
 34. Koralay, H., Arslan, A., Cavdar, S., Ozturk, O., Asikuzun, E., Gunen, A., Tasci, A.T.: *J. Mater. Sci. Mater Electron* **24**, 4270–4278 (2013)